The Journal of Experimental Medicine

Bartonella Adhesin A Mediates a Proangiogenic Host Cell Response

Tanja Riess,[1] Siv G.E. Andersson,[4] Andrei Lupas,[5] Martin Schaller,[2] Andrea Schäfer,[1] Pierre Kyme,[1] Jörg Martin,[5] Joo-Hee Wälzlein,[1] Urs Ehehalt,[1] Hillevi Lindroos,[4] Markus Schirle,[3] Alfred Nordheim,[3] Ingo B. Autenrieth,[1] and Volkhard A.J. Kempf [1]

[1]*Institut für Medizinische Mikrobiologie und Hygiene,* [2]*Universitäts-Hautklinik, and* [3]*Institute for Cell Biology, Department of Molecular Biology, Eberhard-Karls-Universität, 72076 Tübingen, Germany*
[4]*Department of Molecular Evolution, Evolutionary Biology Center, Uppsala University, 75236 Uppsala, Sweden*
[5]*Max-Planck-Institut für Entwicklungsbiologie, 72076 Tübingen, Germany*

Abstract

Bartonella henselae causes vasculoproliferative disorders in humans. We identified a nonfimbrial adhesin of *B. henselae* designated as *Bartonella* adhesin A (BadA). BadA is a 340-kD outer membrane protein encoded by the 9.3-kb *badA* gene. It has a modular structure and contains domains homologous to the *Yersinia enterocolitica* nonfimbrial adhesin (*Yersinia* adhesin A). Expression of BadA was restored in a BadA-deficient transposon mutant by complementation in trans. BadA mediates the binding of *B. henselae* to extracellular matrix proteins and to endothelial cells, possibly via β1 integrins, but prevents phagocytosis. Expression of BadA is crucial for activation of hypoxia-inducible factor 1 in host cells by *B. henselae* and secretion of proangiogenic cytokines (e.g., vascular endothelial growth factor). BadA is immunodominant in *B. henselae*–infected patients and rodents, indicating that it is expressed during *Bartonella* infections. Our results suggest that BadA, the largest characterized bacterial protein thus far, is a major pathogenicity factor of *B. henselae* with a potential role in the induction of vasculoproliferative disorders.

Key words: pilus • endothelial cells • HIF-1 • VEGF • angiogenesis

Introduction

Bartonella henselae is a facultative intracellular bacterium causing cat scratch disease (CSD), bacillary angiomatosis (BA), and bacillary peliosis (BP; reference 1). CSD is a self-limiting disease characterized by lymphadenopathy related to a cat scratch. In immunocompromised individuals, *B. henselae* causes tumorous proliferations of endothelial cells (ECs) in the skin and internal organs, referred to as BA and BP, respectively (2-4).

Stimulation of angiogenesis upon a *Bartonella* infection represents one fascinating feature of human pathogenic bacteria. *Bartonella* species may cause these vasculoproliferations by at least three different mechanisms that may act synergistically: (a) triggering EC proliferation directly (5), (b) inhibition of apoptosis of ECs (6), and (c) induction of the secretion of vasculoproliferative cytokines (e.g., vasculoendothelial growth factor [VEGF]; references 7 and 8). In vivo and in vitro infection with *B. henselae* results in the activation of hypoxia-inducible factor (HIF)-1 (unpublished data), the key transcription factor of angiogenesis (9). The proliferating ECs are one potential habitat of *B. henselae*, as the pathogen survives and replicates within these cells in vitro (10, 11).

Only few bacterial factors operating in *Bartonella*–host cell interactions are known. One of the most important putative pathogenicity factors of *B. henselae* is the "type IV pilus" (12), which mediates host cell adhesion and trigger-

The online version of this article contains supplemental material.

Address correspondence to Volkhard A.J. Kempf, Institut für Medizinische Mikrobiologie und Hygiene, Eberhard-Karls-Universität, Elfriede-Aulhorn-Strasse 6, 72076 Tübingen, Germany. Phone: 49-7071-2981526; Fax: 49-7071-295440; email: volkhard.kempf@med.uni-tuebingen.de

P. Kyme's present address is Centre for Infectious Diseases and Microbiology, University of Sydney, Westmead Hospital, New South Wales 2145, Australia.

Abbreviations used in this paper: ADM, adrenomedullin; BA, bacillary angiomatosis; BadA, *Bartonella* adhesin A; BP, bacillary peliosis; CBA, Columbia blood agar; CLSM, confocal laser scanning microscopy; CSD, cat scratch disease; EC, endothelial cell; ECM, extracellular matrix; Fn, fibronectin; HIF, hypoxia-inducible factor; HMW, high molecular weight; IEM, immunoelectronmicroscopy; IGFBP-3, insulin-like growth factor binding protein 3; NadA, *Neisseria* adhesin A; OMP, outer membrane protein; PFA, paraformaldehyde; TEM, transmission electron microscopy; VEGF, vasculoendothelial growth factor; YadA, *Yersinia* adhesin A.

 J. Exp. Med. © The Rockefeller University Press • 0022-1007/2004/11/1267/12 $8.00
Volume 200, Number 10, November 15, 2004 1267–1278
http://www.jem.org/cgi/doi/10.1084/jem.20040500

Table I. *Bacterial Strains Used in This Study*

Strain	Characteristics	Reference or source
B. henselae		
Wild-type (WT)	*B. henselae* Marseille, patient isolate, early passage	4
Pil$^-$ variant	*B. henselae* Marseille, extensively passaged, pilus-negative	7
BadA$^-$	*B. henselae* Marseille TN <KAN-2> transposon mutant, transposon integrated in *badA*	This study
BadA$^-$/BadA$^+$ WT	*B. henselae* BadA2$^{-/-}$ complemented with pTR15	This study
Houston-1 ATCC 49882	published genome sequence (NC_005956)	24
E. coli		
TOP 10	host strain used for cloning	Invitrogen
DH5α	host strain used for cloning	Invitrogen
BL21 (DE3)	host strain used for protein expression	Stratagene

ing of VEGF secretion (7). "Pilus" expression undergoes phase variation with multiple passages on agar plates (12). Additional candidates in *Bartonella* pathogenicity are outer membrane proteins (OMPs; references 13 and 14) and the *virB* type IV secretion system that is responsible for the inhibition of apoptosis in ECs (15).

Many pathogenic bacteria assemble multifunctional proteinaceous surface structures that serve as adhesins. Such nonfimbrial adhesins, e.g., *Yersinia* adhesin A (YadA) of enteropathogenic *Yersinia* species and *Neisseria* adhesin A (NadA) of *Neisseria meningitidis*, have been described as a novel class of bacterial adhesins representing important pathogenicity factors (16, 17). YadA, the best investigated representative of this protein family, mediates adherence to host cells (18) and extracellular matrix (ECM) proteins (19). YadA expression is essential for pathogenicity of *Yersinia enterocolitica* in a murine infection model (20). Accordingly, NadA is crucial for establishing *N. meningitidis* infection in an infant rat model (17).

Here, we describe the identification, cloning, and characterization of *Bartonella* adhesin A (BadA), formerly known as "type IV pili." The 340-kD BadA protein, encoded by the 9.3-kb *badA* gene, is located in the outer membrane of *B. henselae*. BadA is constructed modularly and contains domains homologous to *Y. enterocolitica* YadA. BadA mediates the binding of *B. henselae* to ECM proteins and ECs, and prevents phagocytosis. It is also crucial for activation of HIF-1 and secretion of VEGF. Moreover, we provide evidence that BadA is expressed during *Bartonella* infections in humans and rodents with implications for serodiagnosis of *Bartonella* infections. Our results suggest that BadA is a major pathogenicity factor of *B. henselae* with a potential role in the induction of the vasculoproliferative disorders BA and BP.

Materials and Methods

Bacteria and Growth Conditions. Bacteria are summarized in Table I. *B. henselae* was grown on Columbia blood agar (CBA) in a humidified atmosphere at 37°C and 5% CO_2. *Escherichia coli* was grown in Luria-Bertani broth. Antibiotics were used at the following concentrations: *B. henselae*: 30 μg/ml kanamycin, 1 μg/ml chloramphenicol; *E. coli*: 50 μg/ml kanamycin, 50 μg/ml chloramphenicol, 100 μg/ml ampicillin.

For production of bacterial stock suspensions, bacteria were harvested from agar plates after 5 d and frozen in Luria-Bertani–20% glycerol at −80°C. The pilus-negative variant strain (*B. henselae* Pil$^-$) was produced by extensively passaging *B. henselae* Marseille WT (7).

SDS-PAGE and Immunoblotting. *B. henselae* were resuspended in SDS sample buffer and heated at 98°C for 3 min. SDS-PAGE was performed in 12% gels. Gels were stained with Coomassie Blue R250. For immunoblotting, proteins were transferred onto nitrocellulose membranes (Schleicher and Schuell). Blots were blocked for 1 h in 5% skim milk powder in 25 mM Tris, pH 7.5, 0.15 M NaCl, and 0.05% Tween 20 (Sigma-Aldrich), and incubated with the respective primary antibody overnight. For detection, a horseradish peroxidase–conjugated secondary antibody was used and signals were visualized either via chemiluminescence (Amersham Biosciences) or with DAB (3,3′-diaminobenzidine tetrahydrochloride; Sigma-Aldrich).

A BadA-specific rabbit antiserum was raised by immunization with a BadA stalk fragment (badA-f6-badA-r6; Table II) and purified by affinity chromatography, a rabbit anti–*B. henselae* Marseille serum was raised by immunization with viable bacteria (11), and a mouse anti–*B. henselae* Marseille serum was raised by immunization with heat-killed bacteria. Human sera were obtained from patients with the clinical diagnosis of CSD and immunoreactivity of >1:200 in an immunofluorescence test according to the recommendations of the Centers of Disease Control (21).

Protein Identification. *B. henselae* was lysed in 7 M urea, 2 M thiourea, and 4% 3-[(3-cholamidopropyl)dimethylammonio]-1-propanesulfonate, and centrifuged at 100,000 *g* for 1 h at 4°C. SDS-PAGE was followed by matrix-assisted laser desorption/ionization peptide mass fingerprinting and electrospray ionization tandem mass spectrometry. In-gel digestion and protein identification with $H_2{}^{18}O$ method was performed as described previously (22). After ZipTip purification (C18-ZipTip; Millipore), aliquots were deposited on α-cyano-4-hydroxycinnamic acid-nitrocellulose for matrix-assisted laser desorption/ionization-time of flight mass analysis (Reflex III; Bruker Daltonic). All measurements were performed in the positive ion reflection mode at an accelerating voltage of 23 kV and delayed-pulsed ion extraction. Sequence verification was performed by nanoelectrospray tandem mass spectrometry on a hybrid quadrupole orthogonal accelera-

Table II. *Plasmids, Primers, and Probes Used in This Study*

Plasmids	Description	Reference or source
pBluescript II KS	cloning vector, Ap^r	Stratagene
pET30b	protein expression vector, Km^r	Novagen
pBBR1MCS	broad host range, Cm^r	46
pTR14	pBluescript II KS containing a 13.2-kb *B. henselae* Marseille EcoRI/ClaI fragment with *badA*, Ap^r	This study
pTR15	pBBR1MCS containing a 13.2-kb BamHI/ClaI fragment of pTR14 with *badA*, Cm^r	This study
pTR52	pET30b containing badA-f6/r6-PCR fragment	This study
Primers		
badA-f2	CTCCAGTCTGATGATTCAGC	This study
badA-r2	GCTATATTGATTTCAGTACCTGC	This study
badA-f6	TGCA*CATATG*AAAGCATTAAGGGGAATGATATCAG[a]	This study
badA-r6	TTAT*CTCGAG*TCAAGTACGCTTATCACTTTTGTTATTAGC[b]	This study
Probe		
pilin	GNTTYTTNAARGAYGARTCNGGNGCANCNGCNATHGARTAYG GNCTNATHGCNGCNTTNATHTCNGT	This study

[a]Italic, NdeI restriction site.
[b]Italic, XhoI restriction site; underline, stop codon.

tion time of flight mass spectrometer (QSTAR Pulsar i; Applied Biosystems). N- versus COOH-terminal peptide sequence orientation was determined using ^{18}O labeling of the COOH termini. MASCOT database searches (National Center for Biotechnology Information [NCBI] nonredundant protein database) used methionine oxidations as variable modifications.

DNA Techniques. Plasmids and primers are listed in Table II. DNA manipulations were performed according to standard protocols.

Transposon Mutagenesis. Transposon mutagenesis was performed by electroporation of the EZ::TN <KAN-2> transposon (EZ::TN <KAN-2> Tnp Transposome Kit; Epicentre) as described previously (23).

Cloning of badA. For construction of pTR14, chromosomal DNA of *B. henselae* Marseille was isolated with QIAGEN Genomic-tip 100/G columns and digested with EcoRI and ClaI, yielding a 13.2-kb fragment containing *badA*, including its putative promoter region according to the sequence of *B. henselae* Houston-1. Fragments larger than 11 kb were ligated into pBluescript II KS and electroporated into *E. coli* TOP 10. The resulting colonies were screened for *badA* by colony blotting using a digoxigenin-labeled *badA* probe (primers: badA-f2 and badA-r2; annealing at 56°C for 30 cycles). Insertion of the 13.2-kb fragment in detected clones was confirmed by sequencing (primers: M13f and M13r; not depicted). The plasmid pTR14 was digested with BamHI and ClaI, and the insert (containing *badA* and the putative promoter region) was ligated into the broad host range vector pBBR1MCS. The resulting plasmid pTR15 was electroporated in *B. henselae* BadA$^-$.

DNA Sequencing Procedures and DNA Sequence Analysis. Parts of the *badA* sequence from *B. henselae* Marseille were obtained by chromosomal sequencing as described previously (23). Additional parts of the sequence were obtained by sequencing of cosmid clones. Clones harboring *badA* were detected from a cosmid library (SuperCos 1 Cosmid Vector Kit; Stratagene) of *B. henselae* Marseille by colony blotting using a *badA* probe (primers: badA-f2 and badA-r2).

The organization of the genomic region of *badA* was examined by PCR in *B. henselae* Marseille WT and *B. henselae* Pil$^-$. Unique PCR primers were designed using the sequence of the homologous region in the Houston-1 strain (sequence data are available from GenBank/EMBL/DDBJ under accession no. NC_005956) as a template (24). PCR products were sequenced (except the highly repetitive inner parts of *badA*) using internal primers and ET terminator chemistry (Amersham Biosciences). Sequences were separated using a MEGABASE sequenator (Amersham Biosciences). GenBank accession numbers are as follows: *B. henselae* Marseille WT, AY560658 (5′ region) and AY560659 (3′ region). The BLAST program of the NCBI (blastn, blastx; http://www.ncbi.nlm.nih.gov) was used to perform sequence similarity searches.

Protein Sequence Analysis. Sequence similarity searches were performed using the programs Blast and PSI-Blast on the nonredundant and microbial genomes databases at the NCBI (http://www.ncbi.nlm.nih.gov). Sequence alignments were made in MACAW (25). Coiled coil segments were predicted using the program COILS (26) and a consensus method based on COILS (unpublished data). Secondary structure predictions were made with PSIPRED (27).

Cloning, Expression, and Purification of a BadA Stalk Fragment. A 480-bp fragment of *badA* encoding for amino acid residues 377–539 (stalk region) was amplified (primers: badA-f6 and badA-r6). The 5′ primer contained an NdeI site and a start codon, and the 3′ primer contained a stop-codon followed by an XhoI site. The fragment was cloned into the expression vector pET30b (Novagen) giving plasmid pTR52. After transformation into *E. coli* BL21 (DE3), expression was induced with 1 mM isopropyl β-D thiogalactopyranoside for 4 h. Cells were lysed in a French press in 30 mM Tris-HCl, pH 7.4, 50 mM NaCl, 5 mM dithiothreitol, 50 μg/ml DNase I, and 1 mM PMSF, and the

protein was purified to homogeneity from the high speed centrifugation supernatant of the lysate by a combination of cation-exchange (MonoS HR; Amersham Biosciences; elution conditions are as follows: 30 mM Tris-maleate, pH 6.0, 5 mM $MgCl_2$, 5 mM dithiothreitol, 0–1 M NaCl gradient) and gel-sizing chromatography (Superdex G-75; Amersham Biosciences; in 50 mM potassium phosphate buffer, pH 7.3, 150 mM NaCl).

Culture and Infection of ECs, J774 Macrophages, and HeLa and GD25 Cells. Human umbilical vein ECs were cultured in EC growth medium (PromoCell). Infection experiments were performed in EC basal medium (PromoCell) as described previously (11). The mouse macrophage cell line J774A.1 (American Type Culture Collection [ATCC] TIB-67) was cultured in RPMI 1640 medium with 10% FCS, 2 mM L-glutamine, 1 mM sodium pyruvate, β-mercaptoethanol, and nonessential amino acids. Macrophages were seeded in 24-well tissue culture plates. HeLa cells were grown in RPMI 1640 with 10% FCS and for infection experiments, media were removed 2 h before infection and replaced by culture media without antibiotics and FCS to avoid unspecific HIF-1 activation. β1 integrin–deficient murine GD25 cells (28) and β1 integrin–overexpressing GD25-β1A cells (29) were cultivated in DMEM (GIBCO BRL) with 10% FCS. For GD25-β1A, 10 μg/ml puromycin (Sigma-Aldrich) was added. In some experiments, *B. henselae* WT and GD25-β1A were preincubated with an anti-fibronectin (Fn) antibody (DakoCytomation).

Bacteria were used at a multiplicity of infection of 100 and sedimented onto cultured cells by centrifugation for 5 min at 300 *g*. The actual inoculum for each experiment was determined by plating serial dilutions and calculating the number of CFUs. For J774 cells, intracellular bacteria were quantified 3 h after infection by gentamicin kill assays as described previously (11).

Determination of B. henselae Binding to ECM Proteins. To assess binding of *B. henselae* to ECM proteins, coverslips were coated with 10 μg/ml human collagen type I, type III (Chemicon), and type IV (Calbiochem), and laminin (Chemicon) and Fn (Sigma-Aldrich). After washing with PBS, 10^7 bacteria were resuspended in 1 ml RPMI 1640 and sedimented on coverslips. After 1 h, coverslips were washed twice with RPMI, fixed with 3.75% PBS-buffered paraformaldehyde (PFA), and bacteria were stained with 1 μg/ml DAPI for 10 min. Adherence was determined via confocal laser scanning microscopy (CLSM) and by counting 20 randomly selected high power fields (1,000-fold magnification).

For detection of Fn binding by Western blotting, bacteria were harvested in PBS and the OD_{550} was adjusted to 1.0. Bacteria were lysed in SDS sample buffer and separated by 12% SDS-PAGE. Membranes were incubated with a monoclonal anti-Fn antibody (Becton Dickinson). Purified human plasma Fn (Chemicon) was used as a positive control (not depicted).

Detection of VEGF, IL-8, Insulin-like Growth Factor Binding Protein 3 (IGFBP-3), and Adrenomedullin (ADM) in Cell Culture Supernatants. Determination of VEGF, IL-8, IGFBP-3, and ADM secretion upon *B. henselae* infection was performed without antibiotics and FCS. 25 ng/ml PMA (Sigma-Aldrich) was used as a positive control (not depicted; reference 7). VEGF concentration in culture medium was measured using a human $VEGF_{165}$-ELISA kit (R&D Systems). IL-8 was determined by ELISA as described previously (30). Secreted IGFBP-3 was measured using a specific RIA (31) and secreted ADM was quantified by a commercially available RIA (Phoenix Pharmaceuticals).

Detection of HIF-1α Activation. For reporter gene assays, a VEGF promoter luciferase reporter construct (pVEGF.4) was used (32). Transfection efficiency was normalized by cotransfection with pCMV β-galactosidase (pCMV β-gal; CLONTECH Laboratories, Inc.). 10^5 HeLa cells were transiently transfected with 0.5 μg pVEGF.4 Luc reporter construct and 0.25 μg pCMV β-gal using ExGen500 transfection reagent (Fermentas), and incubated for 24 h at 37°C. Transfected cells were infected with *B. henselae* or exposed to hypoxia. After 36 h, cells were lysed for determination of Luc activity, protein quantification, and measurement of β-gal using a Luciferase Reporter Gene Assay (Roche). Luminescence was measured with a Topcount scintillation counter (Packard Instrument Co.). Levels of Luc expression were normalized to β-gal activity and total protein concentration (30). Every experiment was performed in quadruplicate. The degree of induction was determined as the ratio of Luc activity of *B. henselae*–infected or hypoxia-exposed cells to that of uninfected control cells.

Immunostaining and CLSM. Bacteria were resuspended in PBS, dried on glass slides, and fixed in 3.75% PBS-buffered PFA. 10^5 ECs were seeded onto coverslips and infection was stopped by 3.75% PFA. Immunostaining of *B. henselae* was performed as described previously (11) using a BadA-specific rabbit antiserum or mouse polyclonal antibodies raised against *B. henselae* Marseille. FITC-conjugated secondary antibodies and TRITC-labeled phalloidin were purchased from Dianova and Sigma-Aldrich. Bacteria were stained with DAPI. Cellular fluorescence was evaluated using a Leica DM IRE 2 CLSM. Three different fluorochromes were detected representing the green (FITC), red (TRITC), and blue (DAPI) channels. Images were digitally processed with Photoshop 6.0 (Adobe Systems). Adherence to ECs and GD25 cells was quantified by counting adherent bacteria from 20 randomly selected cells.

Transmission electron microscopy (TEM) and immunoelectronmicroscopy (IEM). TEM was performed as described previously (11). In brief, *B. henselae* cell pellets were fixed and after embedding in glycide ether, the blocks were cut using an ultra microtome (Ultracut; Reichert). 80-nm ultra-thin sections were stained (Ultrastainer; Leica) with 0.5% uranyl acetate for 10 min at 30°C and 2.7% lead citrate for 5 min at 20°C. For IEM of BadA, post-embedding immunogold labeling was performed. Cells were fixed and after centrifugation, the sediment was embedded in 3% agarose at 37°C and then cooled on ice. Small parts of the agarose blocks were embedded in Lowicryl (Polysciences Ltd.). 50-nm ultra-thin sections were mounted on formvar-coated nickel grids and incubated with anti-BadA rabbit serum, followed by 10 nm gold-conjugated goat anti–rabbit IgG (Auroprobe EM; Amersham Biosciences). In control samples, the primary antibody was omitted. Grids were counterstained with uranyl acetate and lead citrate and examined using a transmission electron microscope (Zeiss EM 109; Carl Zeiss MicroImaging, Inc.).

Statistical Analysis. All experiments were performed at least three times and revealed comparable results. Differences between mean values of experimental and control groups were analyzed by student's *t* test. A p-value of <0.05 was considered statistically significant.

Online Supplemental Material. In Fig. S1, BadA is shown in more detail by electron microscopy (negative staining). In Fig. S2, BadA immunoreactivity of sera from patients suffering from CSD is evaluated by Western blotting of whole cell bacterial lysates. Figs. S1 and S2 are available at http://www.jem.org/cgi/content/full/jem.20040500/DC1.

Results

B. henselae WT, But Not B. henselae Pil⁻ Phase Variant, Binds Fn. To analyze the protein composition of the "pilus"-like structures of *B. henselae*, a comparative protein

analysis of both *B. henselae* WT and a spontaneous *B. henselae* Pil$^-$ variant was performed. TEM revealed no pilus expression of the variant strain (Fig. 1, a and b; reference 7). Expression of "pili" correlated with the observation that bacterial colonies of the WT stuck more tightly to the surface of CBA than Pil$^-$. Protein patterns of whole bacterial lysates (WT and Pil$^-$) showed two high molecular weight (HMW) proteins in *B. henselae* WT (>220 kD) not present in Pil$^-$ (Fig. 1 c). Using electrospray ionization-mass spectrometry/mass spectrometry, the lower band was identified as Fn (not depicted). Analysis of the upper band revealed four peptide fragments (ATN(I/L)(I/L)T(I/L)GK; (I/L)TY(I/L)(I/L)F; AAVT(I/L); and (I/L)YS(I/L)NE(Q/K)(I/L)ATYFG), which matched no entry in the database (blastp; http://www.ncbi.nlm.nih.gov). These were later identified as fragments of BadA (see below). We hypothesized that *B. henselae* WT, but not Pil$^-$, might bind to Fn present in CBA. To further elucidate this hypothesis, Fn binding of *B. henselae* was assessed by Western blotting of whole bacterial lysates and detection of Fn using anti-Fn antibodies. Fn bound to bacteria was detectable in WT, but not in Pil$^-$ lysates (Fig. 1, d and e, lanes 1 and 2). Taken together, the results provide evidence that expression of pilus-like structures on the surface of *B. henselae* is associated with binding to Fn.

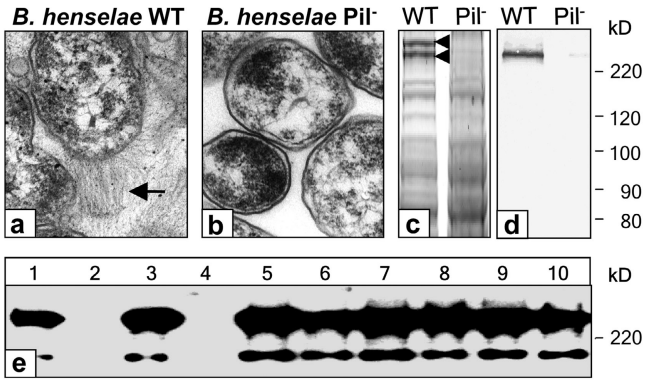

Figure 1. Phase variation of *B. henselae*. (a and b) Expression of so-called type IV-like pili (BadA, arrow; see also Fig. S1, available at http://www.jem.org/cgi/content/full/jem.20040500/DC1) of *B. henselae* Marseille WT not detectable on the surface of *B. henselae* Pil$^-$. (c) SDS-PAGE of *B. henselae* WT and Pil$^-$ showing two differential HMW bands. The lower band is Fn (240 kD), the upper is BadA (calculated mass: 340 kD). (d) Detection of Fn binding of *B. henselae* WT and Pil$^-$ by Western blotting. Bacteria-bound Fn was detected using an anti-Fn antibody. (e) Screening of a *B. henselae* transposon library for Fn binding. *B. henselae* WT (lane 1), Pil$^-$ (lane 2), and transposon mutants (lanes 3–10). Fn binding is not detectable in *B. henselae* Pil$^-$ and in a transposon mutant (lane 4), suggesting loss of BadA (pilus) expression.

Transposon Insertion in badA Results in Loss of Fn Binding. To identify the gene(s) coding for the putative type IV pilus, a transposon library of *B. henselae* Marseille (23) was screened, revealing one transposon mutant (Fig. 1 e, lane 4) deficient in Fn binding, similar to the Pil$^-$ variant described above. By chromosomal sequencing, the site of transposon insertion (nucleotide position 3438) was identified as a 9.3-kb gene of unknown function, based on the genomic sequence of *B. henselae* Houston-1 (24). Database searches revealed protein sequence similarities to hypothetical genes of yet unknown functions in *Brucella melitensis*, *Sinorhizobium meliloti*, and *Mesorhizobium loti* (not depicted). Analysis of the deduced amino acid sequence revealed a protein with a calculated mass of 340 kD, consistent with the size of the differentially expressed upper HMW protein of *B. henselae* WT (Fig. 1 c). The four unidentified peptide fragments mentioned above were present in this translated protein sequence. Protein sequence analysis indicated that this protein belongs to a novel class of nonfimbrial adhesins exemplified by *Yersinia* adhesin A (YadA; reference 16) and *Neisseria* adhesin A (NadA; reference 17). Therefore, we designated the protein *Bartonella* adhesin A (BadA).

BadA Has a Modular Structure and Belongs to the Class of Nonfimbrial Adhesins. BadA shows a high degree of modularity in its domain structure. After a putative signal sequence and a region not similar to any other currently known protein (Fig. 2 a), BadA contains 11 degenerate 14-residue repeats resembling those found in the YadA head sequence (16), which form a novel-type of left-handed β-helix (33). Two of these repeats are interrupted by sequence inserts. At the COOH terminus, after a motif that is highly conserved (often in multiple copies in most nonfimbrial adhesins [16], termed a "neck sequence"), BadA again resembles YadA in the succession of a right-handed coiled coil segment with pentadecad periodicity, a left-handed coiled coil segment with heptad periodicity, and a membrane anchor domain containing four transmembrane β strands. The membrane anchor is thought to form a 12-stranded pore upon trimerization and allow the autotransport of the adhesin across the outer membrane (34). It is conserved in all nonfimbrial adhesins and may represent their defining feature. In between these two N- and COOH-terminal YadA-like regions, BadA contains a single occurrence of a sequence found repetitively in proteins of *Xylella* spp., followed by 21 occasionally truncated copies of a sequence also seen in putative adhesins from uropathogenic and enterohaemorrhagic *E. coli*, *Shigella flexneri*, and *Salmonella* spp. (Fig. 2 b). These central repeats of BadA contain left-handed coiled coil segments and are separated by neck sequences (24 in total). This is the highest number observed in any protein so far. Structurally, the fairly regular alternation of coiled coil and globular sequences suggests an extended, rod-like shape with periodically recurring bulkier and thinner parts, rather like a segmented rope. This conjecture fits well with the great estimated length of BadA (~100–300 nm), as well as its hair-like, flexible appearance in electron micrographs (Fig. 1 a and Fig. S2, available at http://www.jem.org/cgi/content/full/jem.20040500/DC1).

Genomic Organization of the badA Region. The upstream region of the *badA* gene (*B. henselae* Houston-1; gene BH01510) contains three short open reading frames, one of which (BH01500) shows sequence similarity to the 3′ end of *badA*, thought to encode the membrane anchor region (Fig. 2 c). Further upstream is another open reading frame (BH01490) that displays sequence similarity with *badA*

Figure 2. Protein domain structure of BadA and genomic organization of *badA* region. (a) Sequence representation and (b) schematic diagram of the BadA domain structure. Individual domains are color coded. For simplicity, the colors are explained in the figure itself. Regions that could not be assigned by sequence similarity are left black in (a) and shown as open boxes in (b). The sequence is BadA of *B. henselae* Houston-1. Regions also sequenced in *B. henselae* Marseille are marked by black bars in (a) and residues different in the two strains are shown staggered, with the Houston-1 sequence above and the Marseille sequence below. In (b), structurally equivalent regions are connected by gray bars. The organisms are as follows: Bh, *B. henselae*; EcCFT073, *E. coli* strain CFT073; StLT2, *Salmonella typhimurium* strain LT2; Ye, *Y. enterocolitica*. (c) Schematic diagram of the arrangement of genes in a 17.7-kb genomic region of *B. henselae* Houston-1. Details are given in Results. Site of transposon insertion in *B. henselae* Marseille BadA$^-$ and position of the frameshift in the membrane anchor region of *B. henselae* Houston-1 are indicated. Loss of BadA (pilus) expression in a spontaneous *B. henselae* Marseille variant (*B. henselae* Pil$^-$) is correlated with an 8.5-kb deletion (arrow).

(47% over aligned amino acid regions) and also encodes an anchor region. A PCR-based survey revealed an identical gene organization pattern in *B. henselae* Marseille WT. A similar survey of *B. henselae* Marseille Pil$^-$ revealed a large deletion of 8.5 kb spanning from the 5′ terminal end of BH01490 to the 5′ terminal end of *badA*. The deletion seems to have been mediated by repeated sequences present in the beginning of BH01490 and *badA*, resulting in the loss of most of BH01490, the 5′ terminal end of *badA*, and the intergenic segment flanked by these two genes. As a consequence, the 5′ terminal end of BH01490 has fused with a truncated version of *badA* in the Marseille Pil$^-$ strain. Additionally, in the Houston-1 strain there is a 1-bp deletion at the anchor region of *badA* that is not detected in the Marseille strain. As a consequence, the anchor region is not located inside BH01510, but in a separate small gene (BH01520) that is partially overlapping with the 3′ terminal end of BH01510 in the Houston-1 strain. In contrast,

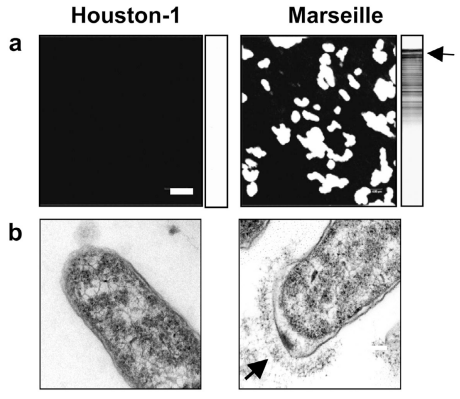

Figure 3. BadA expression of *B. henselae* Houston-1 (ATCC 49882) and *B. henselae* Marseille. (a) BadA expression was analyzed by immunofluorescence and Western blotting using an anti-BadA rabbit serum (arrow). Bar, 2 μm. (b) Detection of BadA expression by TEM. BadA is expressed on the surface of *B. henselae* Marseille (arrow), but missing in the Houston-1 strain (ATCC 49882).

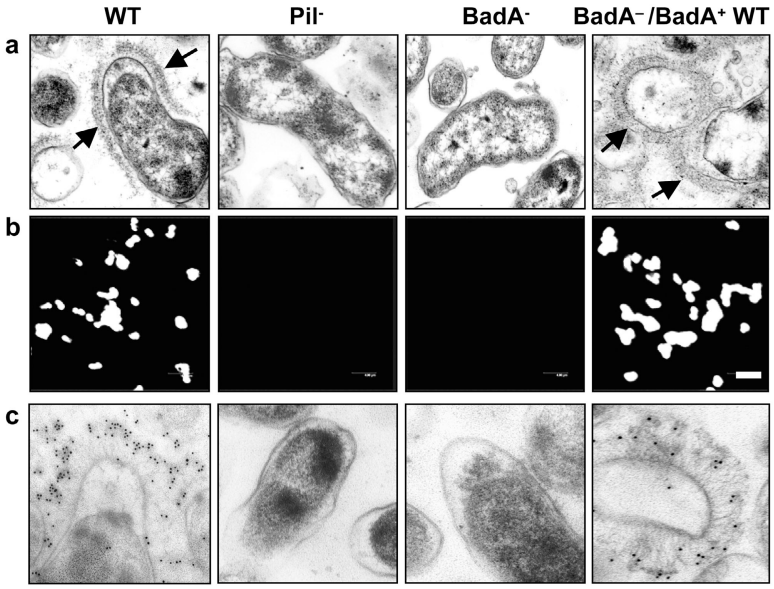

Figure 4. Complementation of *B. henselae* BadA⁻. (a) Detection of BadA expression in *B. henselae* WT, Pil⁻, BadA⁻, and BadA⁻/BadA⁺ WT by TEM. Note the brush-like arrangement of BadA on the surface of the WT and the complemented mutant (arrows) missing in the Pil⁻ variant and the BadA⁻ mutant. (b) Detection of BadA expression by immunofluorescence using an anti-BadA rabbit serum. Bar, 2 μm. (c) Detection of BadA expression by IEM using 10 nm gold-conjugated goat anti–rabbit IgG.

BH01510 and BH01520 are merged into a single gene in the Marseille strain. BadA is expressed in *B. henselae* Marseille, but not in Houston-1 (Fig. 3). From this data we conclude that the *B. henselae* Houston-1 strain we investigated (ATCC 49882) lacks BadA expression.

Complementation of B. henselae BadA⁻ Reveals That BadA Forms the Pilus-like Structure. Complementation of the BadA⁻ mutant was performed with plasmid pTR15 containing a 13.2-kb chromosomal fragment carrying WT *badA*, including its putative promoter region. TEM revealed that expression of BadA in *B. henselae* BadA⁻/BadA⁺ WT leads to the formation of the pilus-like structure (Fig. 4 a). An anti-BadA rabbit serum generated by immunization with a BadA stalk fragment revealed a strong surface staining of the WT and the complemented mutant not detectable in Pil⁻ and BadA⁻ (Fig. 4 b). Consistent data were obtained by IEM showing clearly that BadA is stained (Fig. 4 c). In accordance, this serum was reactive against BadA in OMP preparations of *B. henselae* WT not present in Pil⁻ (not depicted). These results suggest strongly that the formerly described type IV pilus (12) is in fact the non-fimbrial adhesin BadA.

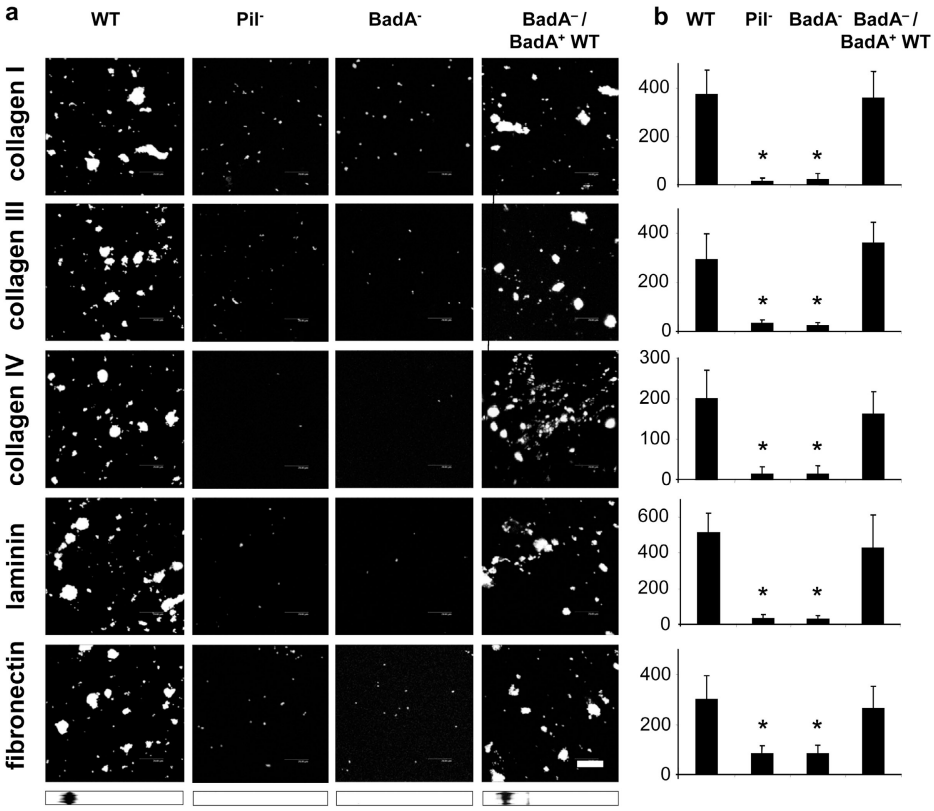

Figure 5. BadA-dependent interaction of *B. henselae* with ECM proteins. Collagen type I, III, and IV, and laminin and Fn binding of *B. henselae* WT, Pil⁻, BadA⁻, and BadA⁻/BadA⁺ WT. (a) Bacteria were seeded onto coated coverslips and DAPI stained. Bar, 20 μm. Fn binding was additionally assessed by Western blotting. (b) Microscopic quantification of bacterial binding to ECM proteins (adherent bacteria per high power field). *, significant difference compared with *B. henselae* WT ($P < 0.01$).

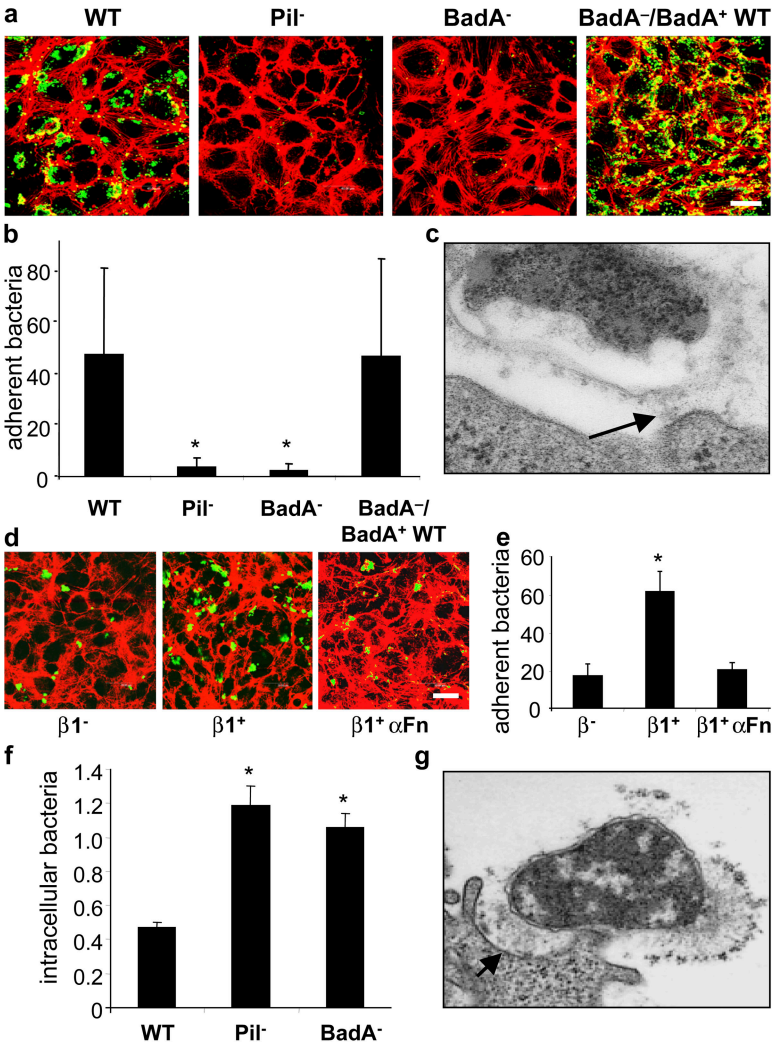

Figure 6. BadA mediates cell adherence and shares antiphagocytic properties. (a) Adherence of *B. henselae* WT, Pil$^-$, BadA$^-$, and BadA$^-$/BadA$^+$ WT to ECs shown by CLSM. Bacteria were labeled by FITC-conjugated antibodies (green signal) and filamentous actin was stained with TRITC-labeled phalloidin (red signal). Bar, 20 μm. (b) Microscopic quantification (bacteria/cell) of EC adherence. (c) Adherence of *B. henselae* WT to ECs shown by TEM. Note that adherence of *B. henselae* WT to the cell surface is mediated via BadA (arrow). (d) Adherence of *B. henselae* WT to GD25 (β1$^-$) and GD25 β1 integrin–overexpressing (β1$^+$) fibroblasts shown by CLSM. For modulation, bacteria and β1$^+$ cells were preincubated with anti-Fn antibodies (β1$^+$ αFN). (e) Microscopic quantification of bacterial adherence to GD25 and GD25 β1 integrin$^+$ fibroblasts. (f) Intracellular *B. henselae* WT, Pil$^-$, and BadA$^-$ 3 h after infection of J774 macrophages. Bacteria (percent of inoculum) were calculated from gentamicin protection assays. (g) Interaction of *B. henselae* WT with J774 macrophages shown by TEM. Note that adherence of *B. henselae* WT to the cell surface is mediated via BadA (arrow). *, Significant difference compared with *B. henselae* WT ($P < 0.01$).

BadA Is Crucial for Interaction of B. henselae with ECM and Host Cells. To investigate whether BadA is involved in binding to ECM proteins, *B. henselae* was exposed to collagen type I, III, and IV, and laminin- and Fn-coated coverslips (Fig. 5). BadA-expressing *B. henselae* WT and BadA$^-$/BadA$^+$ WT bound to a higher degree to these ECM protein–coated surfaces than Pil$^-$ or BadA$^-$. The ability to bind Fn was reconstituted in BadA$^-$/BadA$^+$ WT as additionally shown by Western blotting. From this data we conclude that expression of BadA is crucial for adherence of *B. henselae* to ECM proteins.

Nonfimbrial adhesins mediate adherence of bacteria to host cells (16). As one potential target in *B. henselae* infections is ECs (6, 10, 11), the role of BadA in adherence to these cells was investigated. ECs were infected with *B. henselae* WT, Pil$^-$, BadA$^-$, and BadA$^-$/BadA$^+$ WT and adherence was assessed 30 min after infection by CLSM (Fig. 6, a and b). Both *B. henselae* Pil$^-$ and BadA$^-$ hardly adhered to ECs, showing that BadA expression is crucial for host cell adherence. Consistently, TEM suggests that BadA mediates adherence of *B. henselae* to ECs (Fig. 6 c). Next, we analyzed the role of β1 integrins in the binding of *B. henselae* to host cells, as they mediate YadA-dependent adherence of *Yersinia* (35). For this purpose, the fibroblast cell lines GD25 (lacking β1 integrins; reference 28) and GD25-β1A (overexpressing β1 integrins; reference 29) were infected with *B. henselae* WT. Data revealed a significantly decreased adherence of *B. henselae* WT to GD25, suggesting that β1 integrins act as a cellular binding partner of BadA. This binding might be mediated by Fn, as pretreatment of cells and bacteria with anti-Fn antibodies abolished bacterial adherence to the background level (Fig. 6, d and e). Furthermore, like YadA (36), expression of BadA prevents *B. henselae* WT from phagocytosis in J774 murine macrophages (Fig. 6 f).

Induction of a Proangiogenic Host Cell Response Depends on BadA Expression. HIF-1 is the key transcription factor of angiogenesis regulating, e.g., VEGF, IGFBP-3, and ADM (9). As a *B. henselae* infection activates HIF-1 in host cells (epithelial and endothelial) in vitro and in BA lesions in vivo (unpublished data), we elucidated the role of BadA in this process (Fig. 7 a). HeLa cells were transiently transfected with a VEGF promoter luciferase reporter construct (pVEGF.4; reference 32) specifically regulated by HIF-1.

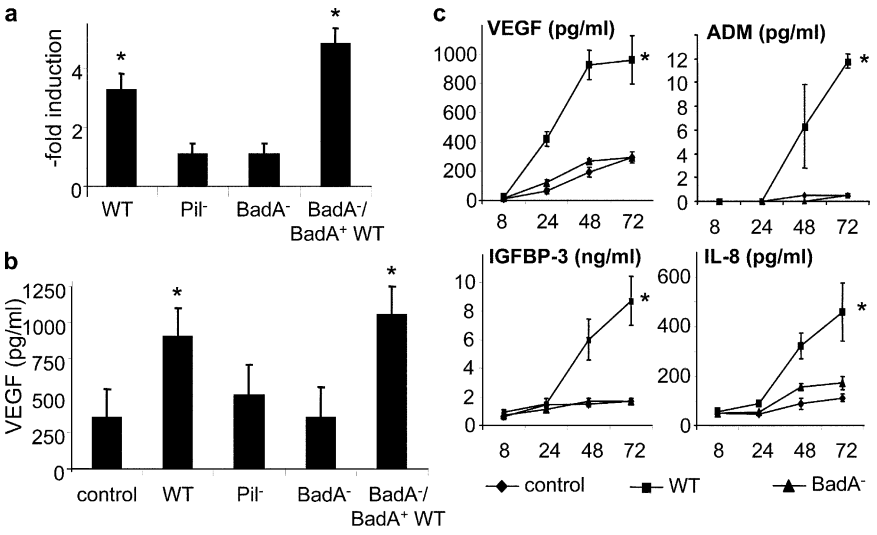

Figure 7. BadA-dependent HIF-1 activation and secretion of proangiogenic cytokines. (a) HIF-1 activation detected by the use of a VEGF promoter luciferase reporter construct (pVEGF.4). HeLa cells were transfected before infection with *B. henselae* WT, Pil$^-$, BadA$^-$, and BadA$^-$/BadA$^+$ WT. Activation was determined by chemiluminescence 36 h after infection. (b) Induction of VEGF secretion upon infection of HeLa cells. Supernatants were taken 48 h after infection and analyzed by ELISA. (c) BadA-dependent secretion of proangiogenic cytokines in Hela cells. Cells were infected with *B. henselae* WT and BadA$^-$, and the amount of secreted VEGF, IGFBP-3, ADM, and IL-8 was determined 8, 24, 48, and 72 h after infection by ELISA or RIA. *, significant difference compared with uninfected control ($P < 0.01$).

Infection with *B. henselae* WT resulted in a 3.3-fold increase in HIF-1–regulated VEGF gene transcription (positive control: hypoxia, 13.2-fold stimulation). Both *B. henselae* Pil$^-$ (1.1-fold) and BadA$^-$ (1.1-fold) did not activate the VEGF promoter in contrast to BadA$^-$/BadA$^+$ WT (4.9-fold). Consistently, secretion of VEGF was fully induced by BadA$^-$/BadA$^+$ WT (Fig. 7 b). Next, the role of BadA in mediating an angiogenic host cell response was investigated. HeLa cells were infected with *B. henselae* WT and BadA$^-$, and secretion of VEGF, ADM, IGFBP-3, and IL-8 was assessed over 72 h (Fig. 7 c). Infection with *B. henselae* WT led to a strong induction of these cytokines, whereas BadA$^-$ failed to induce any of these. From these data we conclude that expression of BadA by *B. henselae* is crucial for the activation of HIF-1 and has major importance in the proangiogenic reprogramming of host cells.

BadA Is an Immunodominant Surface Molecule in B. henselae–infected Patients and Rodents. It has been shown that NadA leads to an anti-NadA immune response in mice (17). Therefore, we were interested in the immunological properties of BadA in *B. henselae* infections (Fig. 8 and Fig. S2). Serum of 7 out of 11 patients suffering from a clinically diagnosed and serologically confirmed CSD (IgG reactivity in immunofluorescence test: 1:200) showed a strong reactivity to BadA identified by Western blots. The BadA-specific bands were absent in *B. henselae* Pil$^-$ (not depicted) and BadA$^-$. The same results were obtained with the serum of a rabbit infected with viable *B. henselae* WT. Anti-BadA reactivity was also seen in sera of mice immunized with heat-killed *B. henselae*. These results suggest that (a) BadA is expressed in vivo in patients suffering from *Bartonella* infections, (b) BadA-specific antibodies are produced in the course of CSD, and (c) that BadA might be a diagnostic marker for the serological diagnosis of *B. henselae* infections.

Discussion

Besides pili, nonpilus-associated adhesins, which are monomeric or oligomeric proteins anchored to the outer membrane, are important bacterial pathogenicity factors. The nonfimbrial adhesins, e.g., YadA of enteropathogenic *Yersinia* species and NadA of *N. meningitidis* represent a novel class of adhesins widely distributed in proteobacteria (16, 17).

BadA Represents a Novel Nonfimbrial Adhesin of B. henselae. The large, filamentous surface structures of *B. henselae* were formerly called type IV pili based on phenotypic and functional properties (adhesion to host cells, autoagglutination; reference 12). Serial passage in vitro leads to a loss of pilus expression in *B. henselae*. However, we have not been able to detect pilin genes in *B. henselae* Marseille using a degenerated probe (Table II) for Southern blotting deduced from *pilA* of *Caulobacter crescentus* (sequence data are avail-

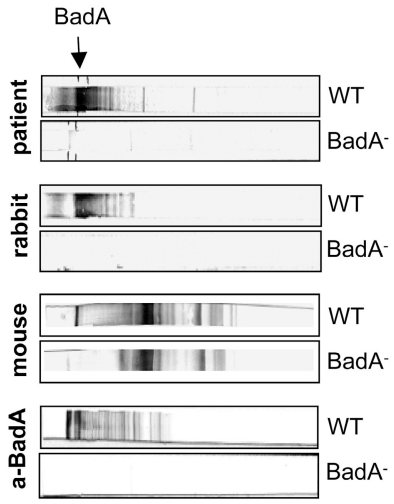

Figure 8. Immunodominance of BadA in humans, rabbits, and mice. Western blots of whole cell lysates of *B. henselae* WT and BadA$^-$ were incubated with serum of a patient suffering from CSD (see also Fig. S2), serum of a rabbit infected with viable *B. henselae*, and serum of a mouse immunized with heat-killed *B. henselae*. The arrow indicates BadA. Note that antibodies against BadA are detected in each of the sera. Immunoreactivity of a specific anti-BadA rabbit serum is shown for control.

able from GenBank/EMBL/DDBJ under accession no. AF_229646), *Agrobacterium tumefaciens* (accession no. AE_007963), *S. meliloti* (accession no. AL_591782), and *M. loti* (accession no. NP_104554; not depicted). Moreover, no pilin genes were found in the *B. henselae* Houston-1 genome sequence (24).

We show that a transposon mutant deficient in expression of the 340-kD BadA was complemented by *badA* (9.3 kb) cloned with its putative promoter region. Our investigations revealed that the so-called type IV pilus of *B. henselae* belongs, like YadA and NadA, to a novel family of nonfimbrial adhesins (16).

B. henselae OMPs have been suggested to be relevant for attachment to ECs (13), induction of a proinflammatory cell response (14), and induction of EC proliferation (5). However, the presence of BadA was not indicated in any of these reports. Reasons for the lack of BadA in the published OMP patterns might be explained by difficulties in gel electrophoresis due to protein size (340 kD) or loss of BadA expression due to extensive passaging and phase variation (7, 12).

Most data on the pathogenicity of *B. henselae* have been obtained using bacteria of variable and unstated passage number. The identification of a deletion mutation in the published genome sequence of the Houston-1 strain and the high density of repeated sequences within the *badA* gene and BH01490, which provides targets for recombination and deletion events, suggests that a high level of variability in sequence and expression among strains is to be expected. Therefore, we recommend that expression of BadA should be evaluated when performing infection experiments with *B. henselae*.

BadA Is an Unusual Representative of the Nonfimbrial Adhesins. Nonfimbrial adhesins share a common architecture, consisting of a head, a stalk, and a membrane anchor (16). This architecture is reflected in a number of broadly occurring sequence motifs, most notably the degenerate 14-residue head repeats, which have been shown in YadA to form a left-handed β-helix (33), the neck sequence, which in YadA separates the head from the stalk and forms a novel trimerization motif (33), and the membrane anchor region, consisting of four transmembrane β strands with potential pore-forming and autotransporter properties (34). All of these motifs are also found in BadA, showing that this protein is a canonical nonfimbrial adhesin. BadA, however, contains additional sequence motifs that have not, so far, been described. Strikingly, these motifs have their closest matches in proteins from γ proteobacteria (*Xylella*, *Escherichia*, *Shigella*, and *Salmonella*), whereas *B. henselae* belongs to the α proteobacteria, suggesting an active "trade" in adhesion domains between phylogenetically distant bacteria. Most conspicuous are segments of ~100 residues, which occur in 21 partly truncated copies in the center of the molecule and are separated from each other by neck sequences. These segments, which contain interspersed coiled coil sequences, account for the surprising size of BadA and probably represent a novel type of stalk architecture judging from electron micrographs. Sequence similarity leads us to expect that similar adhesins will be found on the surface of uropathogenic and enterohaemorrhagic *E. coli* as well as of *Salmonella* spp.

The Role of BadA in the Infection Process. Collagen binding of *Y. enterocolitica* depends on the head repeats of YadA (37). Similar repeats are also present in the BadA head domain and it might be speculated that these motifs mediate adhesion of *B. henselae* to ECM proteins of the basal membrane of blood vessels, which mainly consist of collagen IV and laminin (38), facilitating subsequent infection of ECs. In accordance, adherence of *B. henselae* to collagen type I, III, and IV depends on BadA expression. The molecular basis of the laminin- and Fn-binding capacity of BadA remains unclear. Like YadA (36), BadA shares antiphagocytic capacities, as expression of BadA prevents *B. henselae* from phagocytosis in J774 murine macrophages.

Our data clearly show that expression of BadA is important for adherence of *B. henselae* to ECs that represent one potential habitat (10, 11). It is known that Fn-binding proteins, such as those of *N. meningitidis*, promote the infection process of host cells, possibly via Fn bridging to $\alpha_5\beta_1$ integrins (39). Using β1 integrin–overexpressing GD25 cells and anti-Fn antibodies, we demonstrated that β1 integrins are crucial for cell adhesion of *B. henselae*, possibly via Fn bridging. Our data are also in line with previous reports (35) that show that β1 integrins are required for YadA binding to host cells.

The Role of BadA in the Induction of a Proangiogenic Host Cell Response. HIF-1 is the key transcription factor in angiogenesis (9). Of the many genes induced by HIF, VEGF represents the major mitogen for ECs (40). We and others demonstrated that a *B. henselae* infection results in host cell VEGF secretion in vitro and in BA and BP in vivo (7, 8). Moreover, HIF-1 is activated in host cells by *B. henselae* in vitro and in BA lesions in vivo, and VEGF, IGFBP-3, ADM, and IL-8 (all sharing angiogenic capacities; references 41–43) are secreted in vitro (unpublished data). Our data show that expression of BadA is crucial for both HIF-1 activation and secretion of proangiogenic compounds. Therefore, BadA appears to play a crucial role in the induction of a proangiogenic host cell response. Whether BadA directly triggers expression of proangiogenic factors or mediates adhesion of *B. henselae* to host cells followed by subsequent pathogen–host cell interactions, is not yet clear. Binding of Fn to $\alpha_5\beta_1$ integrins results in activation of a proangiogenic gene expression program (44). One could speculate that BadA might be involved in triggering a proangiogenic host cell response via Fn bridging to $\alpha_5\beta_1$ integrins.

Immunodominance of BadA. Sera of patients suffering from *Bartonella* infection and of rabbits infected with viable *B. henselae* reacted with BadA in immunoblotting (Fig. 8 and Fig. S2), suggesting that BadA is expressed in *B. henselae* infections. The biological functions of BadA expression in vivo might be to avoid phagocytosis similar to YadA (36) and to adhere to ECs. Antibodies against YadA and NadA mediate protection in *Y. enterocolitica* and *N. meningitidis* infections (17, 45). For vaccination strategies against zoonotic *Bartonella* in their mammalian reservoirs, BadA

could therefore be a promising vaccine candidate. The immunodominance of BadA in the sera of *B. henselae*–infected patients suggests also that it might be a suitable marker for serodiagnosis of *B. henselae* infections.

In conclusion, the nonfimbrial adhesin BadA is (a) an unusual modularly constructed, surface-exposed HMW protein, (b) highly important for pathogen–host cell interactions, (c) involved in the induction of a proangiogenic host cell response, and (d) an immunodominant antigen. Further investigations will elucidate the role of this multifunctional molecule in *Bartonella* infections.

We thank B. Schütt for performing IGFBP-3 and ADM RIAs. We also thank A. Roggenkamp, J. Heesemann, K. Alitalo, and C. Wolz for helpful discussions and D. Neumann, E. Januschke, B. Fehrenbacher, L. Nirell, K. Strijbis, A.-S. Eriksson, and A. Ursinus for excellent technical assistance.

The work of V.A.J. Kempf was supported by grants from the Deutsche Forschungsgemeinschaft (DFG), the "Landesforschungsschwerpunktprogramm" of the Ministry of Science, Research and Arts Baden-Württemberg, and from the University of Tübingen (*Fortüne*-Programm). The work of S.G.E. Andersson was supported from the Wallenberg Foundation, the Foundation for Strategic Research, and the Swedish Research Council. A. Nordheim is supported by the DFG, the MWK Stuttgart, and the Fonds der Chemischen Industrie.

The authors have no conflicting financial interests.

Submitted: 16 March 2004
Accepted: 15 September 2004

References

1. Anderson, B.E., and M.A. Neuman. 1997. *Bartonella* spp. as emerging human pathogens. *Clin. Microbiol. Rev.* 10:203–219.
2. Relman, D.A., J.S. Loutit, T.M. Schmidt, S. Falkow, and L.S. Tompkins. 1990. The agent of bacillary angiomatosis. An approach to the identification of uncultured pathogens. *N. Engl. J. Med.* 323:1573–1580.
3. Koehler, J.E., F.D. Quinn, T.G. Berger, P.E. LeBoit, and J.W. Tappero. 1992. Isolation of *Rochalimaea* species from cutaneous and osseous lesions of bacillary angiomatosis. *N. Engl. J. Med.* 327:1625–1631.
4. Drancourt, M., R. Birtles, G. Chaumentin, F. Vandenesch, J. Etienne, and D. Raoult. 1996. New serotype of *Bartonella henselae* in endocarditis and cat-scratch disease. *Lancet*. 347: 441–443.
5. Conley, T., L. Slater, and K. Hamilton. 1994. *Rochalimaea* species stimulate human endothelial cell proliferation and migration in vitro. *J. Lab. Clin. Med.* 124:521–528.
6. Kirby, J.E., and D.M. Nekorchuk. 2002. *Bartonella*-associated endothelial proliferation depends on inhibition of apoptosis. *Proc. Natl. Acad. Sci. USA*. 99:4656–4661.
7. Kempf, V.A., B. Volkmann, M. Schaller, C.A. Sander, K. Alitalo, T. Riess, and I.B. Autenrieth. 2001. Evidence of a leading role for VEGF in *Bartonella henselae*-induced endothelial cell proliferations. *Cell. Microbiol.* 3:623–632.
8. Resto-Ruiz, S.I., M. Schmiederer, D. Sweger, C. Newton, T.W. Klein, H. Friedman, and B.E. Anderson. 2002. Induction of a potential paracrine angiogenic loop between human THP-1 macrophages and human microvascular endothelial cells during *Bartonella henselae* infection. *Infect. Immun.* 70: 4564–4570.
9. Pugh, C.W., and P.J. Ratcliffe. 2003. Regulation of angiogenesis by hypoxia: role of the HIF system. *Nat. Med.* 9:677–684.
10. Brouqui, P., and D. Raoult. 1996. *Bartonella quintana* invades and multiplies within endothelial cells *in vitro* and *in vivo* and forms intracellular blebs. *Res. Microbiol.* 147:719–731.
11. Kempf, V.A., M. Schaller, S. Behrendt, B. Volkmann, M. Aepfelbacher, I. Cakman, and I.B. Autenrieth. 2000. Interaction of *Bartonella henselae* with endothelial cells results in rapid bacterial rRNA synthesis and replication. *Cell. Microbiol.* 2:431–441.
12. Batterman, H.J., J.A. Peek, J.S. Loutit, S. Falkow, and L.S. Tompkins. 1995. *Bartonella henselae* and *Bartonella quintana* adherence to and entry into cultured human epithelial cells. *Infect. Immun.* 63:4553–4556.
13. Burgess, A.W., and B.E. Anderson. 1998. Outer membrane proteins of *Bartonella henselae* and their interaction with human endothelial cells. *Microb. Pathog.* 25:157–164.
14. Fuhrmann, O., M. Arvand, A. Gohler, M. Schmid, M. Krull, S. Hippenstiel, J. Seybold, C. Dehio, and N. Suttorp. 2001. *Bartonella henselae* induces NF-kappaB-dependent upregulation of adhesion molecules in cultured human endothelial cells: possible role of outer membrane proteins as pathogenic factors. *Infect. Immun.* 69:5088–5097.
15. Schmid, M.C., R. Schulein, M. Dehio, G. Denecker, I. Carena, and C. Dehio. 2004. The VirB type IV secretion system of *Bartonella henselae* mediates invasion, proinflammatory activation and antiapoptotic protection of endothelial cells. *Mol. Microbiol.* 52:81–92.
16. Hoiczyk, E., A. Roggenkamp, M. Reichenbecher, A. Lupas, and J. Heesemann. 2000. Structure and sequence analysis of *Yersinia* YadA and *Moraxella* UspAs reveal a novel class of adhesins. *EMBO J.* 19:5989–5999.
17. Comanducci, M., S. Bambini, B. Brunelli, J. Adu-Bobie, B. Arico, B. Capecchi, M.M. Giuliani, V. Masignani, L. Santini, S. Savino, et al. 2002. NadA, a novel vaccine candidate of *Neisseria meningitidis*. *J. Exp. Med.* 195:1445–1454.
18. Roggenkamp, A., K. Ruckdeschel, L. Leitritz, R. Schmitt, and J. Heesemann. 1996. Deletion of amino acids 29 to 81 in adhesion protein YadA of *Yersinia enterocolitica* serotype O:8 results in selective abrogation of adherence to neutrophils. *Infect. Immun.* 64:2506–2514.
19. Schulze-Koops, H., H. Burkhardt, J. Heesemann, K. von der Mark, and F. Emmrich. 1992. Plasmid-encoded outer membrane protein YadA mediates specific binding of enteropathogenic yersiniae to various types of collagen. *Infect. Immun.* 60:2153–2159.
20. Pepe, J.C., M.R. Wachtel, E. Wagar, and V.L. Miller. 1995. Pathogenesis of defined invasion mutants of *Yersinia enterocolitica* in a BALB/c mouse model of infection. *Infect. Immun.* 63:4837–4848.
21. Serodiagnosis of Emerging Infectious Diseases. *Bartonella* and *Ehrlichia* Infections (course manual). 1999. Centers of Disease Control and Prevention. Atlanta, USA.
22. Shevchenko, A., I. Chernushevich, W. Ens, K.G. Standing, B. Thomson, M. Wilm, and M. Mann. 1997. Rapid 'de novo' peptide sequencing by a combination of nanoelectrospray, isotopic labeling and a quadrupole/time-of-flight mass spectrometer. *Rapid Commun. Mass Spectrom.* 11:1015–1024.
23. Riess, T., B. Anderson, A. Fackelmayer, I.B. Autenrieth, and V.A. Kempf. 2003. Rapid and efficient transposon mutagenesis of *Bartonella henselae* by transposome technology. *Gene*. 313:103–109.

24. Alsmark, C.M., A.C. Frank, E.O. Karlberg, B.A. Legault, D.H. Ardell, B. Canback, A.S. Eriksson, A.K. Naslund, S.A. Handley, M. Huvet, et al. 2004. The louse-borne human pathogen *Bartonella quintana* is a genomic derivative of the zoonotic agent *Bartonella henselae*. *Proc. Natl. Acad. Sci. USA.* 101:9716–9721.
25. Schuler, G.D., S.F. Altschul, and D.J. Lipman. 1991. A workbench for multiple alignment construction and analysis. *Proteins.* 9:180–190.
26. Lupas, A., M. Van Dyke, and J. Stock. 1991. Predicting coiled coils from protein sequences. *Science.* 252:1162–1164.
27. McGuffin, L.J., K. Bryson, and D.T. Jones. 2000. The PSIPRED protein structure prediction server. *Bioinformatics.* 16:404–405.
28. Fassler, R., M. Pfaff, J. Murphy, A.A. Noegel, S. Johansson, R. Timpl, and R. Albrecht. 1995. Lack of beta 1 integrin gene in embryonic stem cells affects morphology, adhesion, and migration but not integration into the inner cell mass of blastocysts. *J. Cell Biol.* 128:979–988.
29. Wennerberg, K., L. Lohikangas, D. Gullberg, M. Pfaff, S. Johansson, and R. Fassler. 1996. Beta 1 integrin-dependent and -independent polymerization of fibronectin. *J. Cell Biol.* 132: 227–238.
30. Schulte, R., G.A. Grassl, S. Preger, S. Fessele, C.A. Jacobi, M. Schaller, P.J. Nelson, and I.B. Autenrieth. 2000. *Yersinia enterocolitica* invasin protein triggers IL-8 production in epithelial cells via activation of Rel p65-p65 homodimers. *FASEB J.* 14:1471–1484.
31. Blum, W.F., M.B. Ranke, K. Kietzmann, E. Gauggel, H.J. Zeisel, and J.R. Bierich. 1990. A specific radioimmunoassay for the growth hormone (GH)-dependent somatomedin-binding protein: its use for diagnosis of GH deficiency. *J. Clin. Endocrinol. Metab.* 70:1292–1298.
32. Ikeda, E., M.G. Achen, G. Breier, and W. Risau. 1995. Hypoxia-induced transcriptional activation and increased mRNA stability of vascular endothelial growth factor in C6 glioma cells. *J. Biol. Chem.* 270:19761–19766.
33. Nummelin, H., M.C. Merckel, J.C. Leo, H. Lankinen, M. Skurnik, and A. Goldman. 2004. The *Yersinia* adhesin YadA collagen-binding domain structure is a novel left-handed parallel beta-roll. *EMBO J.* 23:701–711.
34. Roggenkamp, A., N. Ackermann, C.A. Jacobi, K. Truelzsch, H. Hoffmann, and J. Heesemann. 2003. Molecular analysis of transport and oligomerization of the *Yersinia enterocolitica* adhesin YadA. *J. Bacteriol.* 185:3735–3744.
35. Bliska, J.B., M.C. Copass, and S. Falkow. 1993. The *Yersinia pseudotuberculosis* adhesin YadA mediates intimate bacterial attachment to and entry into HEp-2 cells. *Infect. Immun.* 61: 3914–3921.
36. China, B., B.T. N'Guyen, M. de Bruyere, and G.R. Cornelis. 1994. Role of YadA in resistance of *Yersinia enterocolitica* to phagocytosis by human polymorphonuclear leukocytes. *Infect. Immun.* 62:1275–1281.
37. El Tahir, Y., and M. Skurnik. 2001. YadA, the multifaceted *Yersinia* adhesin. *Int. J. Med. Microbiol.* 291:209–218.
38. Yurchenco, P.D., and J.C. Schittny. 1990. Molecular architecture of basement membranes. *FASEB J.* 4:1577–1590.
39. Unkmeir, A., K. Latsch, G. Dietrich, E. Wintermeyer, B. Schinke, S. Schwender, K.S. Kim, M. Eigenthaler, and M. Frosch. 2002. Fibronectin mediates Opc-dependent internalization of *Neisseria meningitidis* in human brain microvascular endothelial cells. *Mol. Microbiol.* 46:933–946.
40. Yancopoulos, G.D., S. Davis, N.W. Gale, J.S. Rudge, S.J. Wiegand, and J. Holash. 2000. Vascular-specific growth factors and blood vessel formation. *Nature.* 407:242–248.
41. Oehler, M.K., S. Hague, M.C. Rees, and R. Bicknell. 2002. Adrenomedullin promotes formation of xenografted endometrial tumors by stimulation of autocrine growth and angiogenesis. *Oncogene.* 21:2815–2821.
42. Schmid, M.C., M. Bisoffi, A. Wetterwald, E. Gautschi, G.N. Thalmann, S. Mitola, F. Bussolino, and M.G. Cecchini. 2003. Insulin-like growth factor binding protein-3 is overexpressed in endothelial cells of mouse breast tumor vessels. *Int. J. Cancer.* 103:577–586.
43. Koch, A.E., P.J. Polverini, S.L. Kunkel, L.A. Harlow, L.A. DiPietro, V.M. Elner, S.G. Elner, and R.M. Strieter. 1992. Interleukin-8 as a macrophage-derived mediator of angiogenesis. *Science.* 258:1798–1801.
44. Klein, S., A.R. de Fougerolles, P. Blaikie, L. Khan, A. Pepe, C.D. Green, V. Koteliansky, and F.G. Giancotti. 2002. Alpha 5 beta 1 integrin activates an NF-kappa B-dependent program of gene expression important for angiogenesis and inflammation. *Mol. Cell. Biol.* 22:5912–5922.
45. Vogel, U., I.B. Autenrieth, R. Berner, and J. Heesemann. 1993. Role of plasmid-encoded antigens of *Yersinia enterocolitica* in humoral immunity against secondary *Y. enterocolitica* infection in mice. *Microb. Pathog.* 15:23–36.
46. Kovach, M.E., R.W. Phillips, P.H. Elzer, R.M. Roop, and K.M. Peterson. 1994. pBBR1MCS: a broad-host-range cloning vector. *Biotechniques.* 16:800–802.